Multi-objective optimization of electronics heat sinks cooled by natural convection

2016 J. Phys.: Conf. Ser. 745 032068

(http://iopscience.iop.org/1742-6596/745/3/032068)

Multi-objective optimization of electronics heat sinks cooled by natural convection

K Lampio, R Karvinen
Tampere University of Technology, P.O. Box 589, Tampere FI-33101, Finland

E-mail: kaj.lampio@tut.fi

Abstract. Fins and fin arrays with constant temperature at the fin base have known solutions for natural convection. However, in practical applications, no simple solution exists for maximum temperature of heat sink with many heat dissipating components located at the base plate. A calculation model is introduced here to solve this practical problem without time consuming CFD modelling of fluid flow and heat transfer. Solutions with the new model are compared with some simple analytical and CFD solutions to prove that the results are accurate enough for practical applications. Seminal here is that results are obtained many orders of magnitude faster than with CFD. This much shorter calculation time scale makes the model well suited for multi-objective optimization in, e.g., simultaneous minimization of heat sink maximum temperature, size, and mass. An optimization case is presented in which heat sink mass and size are significantly reduced over those of the original reference heat sink.

1. Introduction

Natural convection is used in electronics cooling, especially when reliability or low noise level is required. One such application is the mobile phone base station, where forced convection should be replaced with natural convection to avoid possible fan failure. Natural convection heat sinks have a limited cooling rate, and optimization is necessary in their design to maintain their maximum temperatures and the heat sink outer dimensions within specified limits.

Natural convection heat sinks were first studied in the 1940s by Elenbaas [1], who developed a model based on asymptotic solutions of developing and fully developed flow. Elenbaas also discovered that combined forced convection results of the friction factor f and the Reynolds number Re could be used as part of the Nusselt number correlation in natural convection. Later, his Nusselt number results were correlated in an easy-to-use Nusselt number formula by Bar-Cohen and Rohsenow [2].

Elenbaas's model and the idea of using forced convection friction factor results were reviewed and refined by Aihira [3] and Raithby and Hollands [4], who introduced the Nusselt number for isothermal channels with arbitrary cross sections and used the fRe product as part of their model. Their model was further refined by Yovanovich and Teertstra [5], who used the square root of the cross sectional area as a characteristic length. Results of forced convection were also used in [6], which presents an approximate method to take into account an arbitrarily varying surface temperature.

All the above studies deal with isothermal fins, channels, or base plates, but no solution exists for heat dissipating components at arbitrary locations on a base plate. This paper presents a model that can be used in optimization of practical industrial applications containing multiple discrete heat sources on their base plate. Our optimization method is the same as that used for forced convection in [7,8].

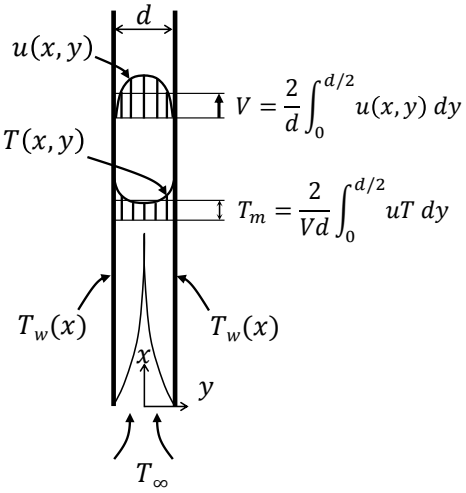

Figure 1. Schematics of a channel

2. Details of the heat transfer model

One-dimensional momentum and energy equations are used. Buoyancy effects are taken into account with the Boussinesq approximation. Because heat sinks comprise many parallel fins and are usually made of low emissivity aluminium, thermal radiation can be ignored (see figures 2 and 7). Only convective heat transfer between the fin surface and fluid, and conduction in a solid are needed in the model.

2.1. Fluid momentum equation

If we assume a channel much taller in comparison to its width, the velocity field of the channel (see figure 1) in steady state natural convection flow with the Boussinesq approximation is governed by the equation

$$\upsilon\frac{\partial^2 u}{\partial y^2}=\frac{1}{\rho}\frac{dp}{dx}+g=-g\beta\left(T_{ave}-T_{\infty}\right), \tag{1}$$

where T_{ave} is the average fluid temperature in a channel defined in (6), $\beta = 1/T_{\infty}$ is the thermal expansion coefficient, and ν kinematic viscosity. On the other hand, shear stress is assumed to follow the equation for internal forced flow

$$\upsilon\frac{\partial^2 u}{\partial y^2}=\frac{1}{\rho}\frac{\partial p}{\partial x}=-\frac{1}{2}V^2\frac{4f}{d_h}, \tag{2}$$

where the mean friction factor is defined as

$$f=\frac{\tau_s}{\frac{1}{2}\rho V^2}. \tag{3}$$

Combining (1), (2), and (3), the mean velocity is

$$V=\frac{g\beta d_h^2}{2\upsilon\left(f\,\mathrm{Re}\right)}\left(T_{ave}-T_{\infty}\right), \tag{4}$$

where the Reynolds number is

$$\mathrm{Re} = \frac{Vd_h}{\upsilon} \tag{5}$$

and the hydraulic diameter is $d_h = 2d$ in the channel in figure 1. In above equations, T_{ave} is the average fluid temperature in a channel, and it is obtained from the local mean temperature $T_m(x)$

$$T_{ave} = \frac{1}{L}\int_0^L T_m(x)dx\,. \tag{6}$$

If the surface temperature in figure 1 is constant and equal to T_w, we have an isothermal surface. In a long channel T_{ave} equals T_w. This approach has been used in the literature for solving heat transfer from natural convection cooled channels with isothermal walls.

The mean *f*Re product in (4) is calculated from the result of a laminar forced flow between parallel plates [8]

$$f\,\mathrm{Re} = 3.44(x^+)^{-0,5} + \frac{\frac{0.647}{4x^+} + 24 - 3.44(x^+)^{-0,5}}{1 + 0.000029(x^+)^{-2}}, \quad x^+ = \frac{x}{\mathrm{Re}\,d_h}\,. \tag{7}$$

2.2. Fluid energy equation

A change in the mixed mean temperature in a channel is obtained from the equation

$$\rho c_p VA\frac{\partial T_m(x)}{\partial x} = h(x)\left[T_w(x) - T_m(x)\right], \tag{8}$$

where $h(x)$, $T_w(x)$ and $T_m(x)$ *are* local values of the heat transfer coefficient, wall, and mixed mean temperatures, respectively. In the solution procedure, the mixed mean temperature can be integrated within a single control volume. The exiting mean temperature $T_{m,out}$ in a Δx long control volume is

$$\frac{T_{m,out} - T_w}{T_{m,in} - T_w} = \exp(-C), \tag{9}$$

where $T_{m,in}$ is the entering mean temperature and C is

$$C = \frac{\int_x^{x+\Delta x} 4h(x)dx}{\rho c_p V d_h}, \tag{10}$$

where c_p is the fluid specific heat and h(x) is the local heat transfer coefficient, which can be obtained from equation [9]:

$$Nu = \frac{h(x)d_h}{k} = 7.541 + 6.874(1000x^*)^{-0.488}e^{-245x^*}, \quad x^* = \frac{x}{\mathrm{Re}\,\mathrm{Pr}\,d_h} \geq 0.001. \tag{11}$$

2.3. Conduction in a fin and base plate

The energy equation of a fin and base plate is (see figure 2)

$$\frac{\partial^2 T}{\partial x^2} + \frac{\partial^2 T}{\partial y^2} + \frac{\partial^2 T}{\partial z^2} = 0\,. \tag{12}$$

Convection and conduction are coupled by the equation

$$q = h(x)\left[T_w(x) - T_m(x)\right], \tag{13}$$

where the local heat flux q is obtained from the solution of (12). Fins can be treated using a 2D approach, but in the base plate, heat conduction is three-dimensional.

2.4. Algorithm

1. Initial guess of average fluid temperature T_{ave} and $T_w(x)$ distribution.
2. Mean velocity V from (5), $f\,\mathrm{Re}$ from (7).
3. $T_m(x)$ from (9), for which $h(x)$ is obtained from (11).
4. New $T_w(x)$ distribution by solving the heat conduction in the walls and in the base plate using the finite volume method and combining it with the heat flux from walls to fluid from (13).
5. Upgrading the average fluid temperature T_{ave} from $T(x)$ values using (7).
6. If T_{ave} differs from the previous value, calculation is repeated starting from point 2.

The solution method is discussed in detail in ref. [7], which introduces the procedure to solve forced convection heat transfer in a fin array.

3. Testing the new model

The model was tested by comparing its results with those of a single isothermal 2D channel and two full scale 3D heat sinks, described below.

3.1. Isothermal 2D-channel

The mean Nusselt number of an isothermal vertical channel with natural convection was presented by Bar-Cohen [2]

$$\mathrm{Nu} = \frac{hd}{k} = \left(\frac{576}{\mathrm{El}^2} + \frac{2.873}{\sqrt{\mathrm{El}}}\right)^{-1/2}, \qquad \mathrm{El} = \frac{g\beta(T_w - T_\infty)d^3}{\upsilon^2}\mathrm{Pr}\frac{d}{L}, \tag{14}$$

where El is the Elenbaas number. The total heat transfer rate from an isothermal channel is

$$\phi_{ic} = 2hLl\left(T_w - T_\infty\right). \tag{15}$$

An isothermal 2D channel was calculated using the new model and different combinations of geometry and temperature, shown in table 1. The results of our model are given in figure 3. The figure shows also the results of CFD calculations and the Bar-Cohen equation (14). Modelling was performed using the open source CFD software OpenFOAM with a compressible (ideal gas law) flow solver (buoyantPimpleFoam), laminar, 2D flow, the Sutherland viscosity law, and Pr = 0.7 and c_p = 1006 J/kgK.

Table 1. Dimensions and temperatures of the tested 2D channel

Dimension	Value	Unit
L	50; 100; 200; 400	mm
d	5; 7.5; 10; 15	mm
T_w	310; 320; 330	K
T_∞	280; 290; 300	K

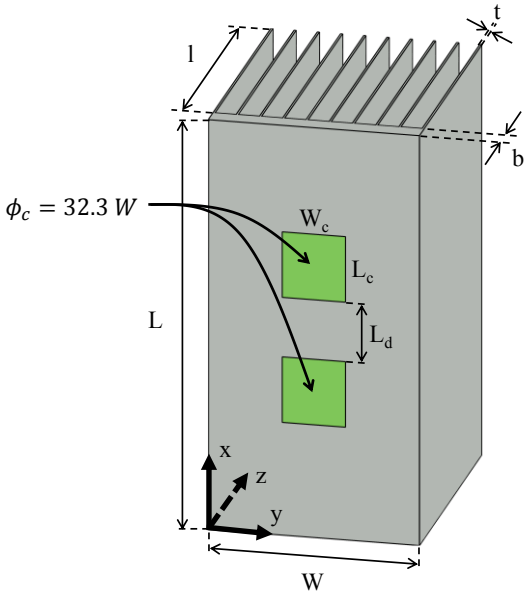

Dimension	Value [mm]
L	200
l	120
W	100
b	10
t	1
L_c	32
W_c	30
L_d	24

Figure 2. Setup and dimensions of the tested 3D heat sink

3.2. Full scale 3D heat sinks

Full scale 3D heat sink calculations were also done with CFD (OpenFOAM). The solver was chtMultiRegionFoam, which is suitable for conjugated heat transfer. The temperature fields of solid and fluid were modelled as separate regions and coupled at the fluid-solid interfaces. The total number of cells in the 3D calculation was around 10^6 for the fluid and 5 x 10^4 for the solid region. A transient solution was necessary to maintain a stable solution. In transient numerical modelling, time step is usually controlled with the Courant-Friedrichs-Levy condition (CFL, also referred to as the Courant number). The global maximum time step value Δt was controlled with

$$CFL = \frac{|\bar{V}|\Delta t}{\Delta x} \leq CFL_{\max}. \tag{16}$$

The maximum CFL number was calculated for the whole field, and the time step was set globally to this limiting value for every cell. The CFL should be smaller than 1.

Instead of a global maximum time step, a local time step (LTS) can also be used. This solution method reaches a steady state solution faster than a pure transient solution. In the LTS, the CFL condition is also used to calculate the maximum time step for each cell individually, a procedure that results in different time step lengths for different cells. We adopted here the LTS solution and tested it on the reference array in figure 2. The results are the same as with the traditional transient solution, but they required less CPU time.

4. Testing the accuracy of the new model

Verification results are first presented for the isothermal 2D channel and then for the full scale 3D heat sink.

4.1. Isothermal 2D channel

Results of our new model, CFD, and those of Bar-Cohen are shown in figure 3 for the 2D channel (see table 1). For clarity reasons only a portion of the 144 combinations from table 1 are shown in the figure. These results are in good agreement, and the most noticeable detail is that the Nusselt numbers calculated with the new model tend to be slightly higher than those of CFD.

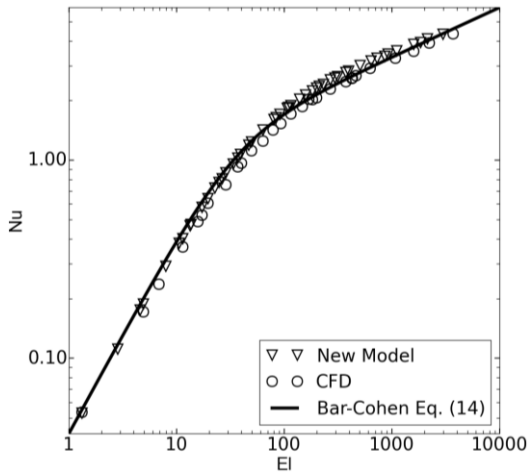

Figure 3. Results by different methods on an isothermal 2D channel.

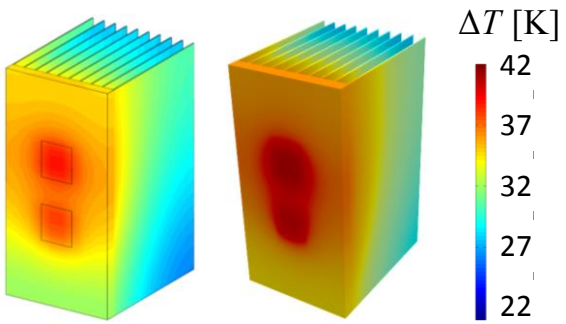

Figure 4. Temperature field of the new model (left) and CFD (right).

4.2. Full scale 3D heat sink

Results of the new model and CFD for the reference 3D fin array are shown in figure 4. Compared to the CFD result, the new model predicts the maximum temperature, the most interesting variable in terms of thermal management, quite well. Table 2 shows numerical values between the minimum and maximum temperature differences. The main advantage of the new model is its faster calculation of one solution of fixed array geometry: 1 – 5 seconds (with 1 core) as opposed to about 5000 seconds with the LTS CFD solution (with 4 cores). The similarity of results and the significantly shorter solution time makes the model well suited for industrial optimization. As an additive side note, real arrays can, indeed, be modelled with 2D CFD calculations if temperature fields are the main concern. If modelling is made in 3D, it affects noticeably only the flow field in the region near the fin tips and outside the array.

Table 2. Minimum and maximum temperature difference (from figure 4)

	CFD	Model	Difference
$\Delta T_{\min}$	23.5	21.4	-8.9 %
$\Delta T_{\max}$	41.7	38.9	-6.7 %

5. Multi-objective optimization

An optimization method similar to that used for forced convection cooling in [7] and [8] was applied to a natural convection heat sink in figure 2. A constrained optimization problem is solved using an exterior penalty function. In this method, the object function $f_i(\mathbf{x})$ is replaced with $F_i(\mathbf{x})$:

$$F_i(\mathbf{x}) = \begin{cases} f_i(\mathbf{x}) & \mathbf{x} \in \Omega \\ f_{\max} + \sum_{i=1}^{n_{ie}} \max[0, g_i(\mathbf{x})] & \text{otherwise} \end{cases}.$$

The evaluation differs from $f_i(\mathbf{x})$ in those solutions that are not located within a feasible area. For those solutions, a penalty constant $f_{\max}$, which is larger than maximum value of any objective function, and sum of active inequality functions, is evaluated as function value.

The multi-objective optimization algorithm we used was a slightly modified MOPSO algorithm presented in [10]. The variables in optimization were the geometrical parameters of a fin array *W, L, l, t, b*, the number of fins *N*, and the component locations on the base plate (see figure 2). The outer

volume of the heat sink and its material weight were chosen as objectives and they were optimized simultaneously. More details of the whole procedure can be found in [7].

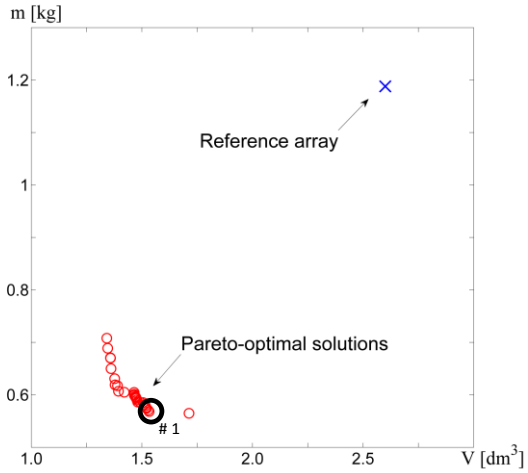

Figure 5. Pareto-Optimal solutions

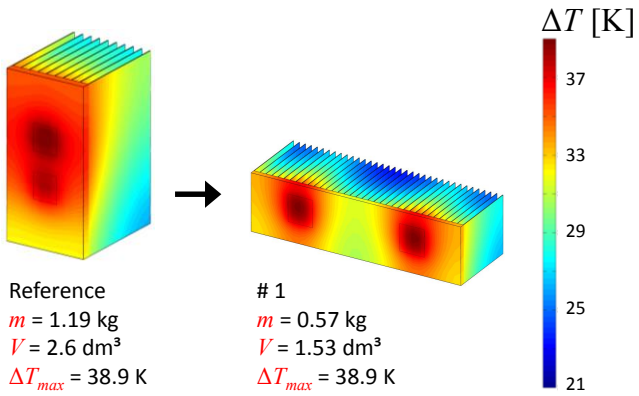

Figure 6. Reference and optimized solution #1 (from figure 5) calculated with the new model

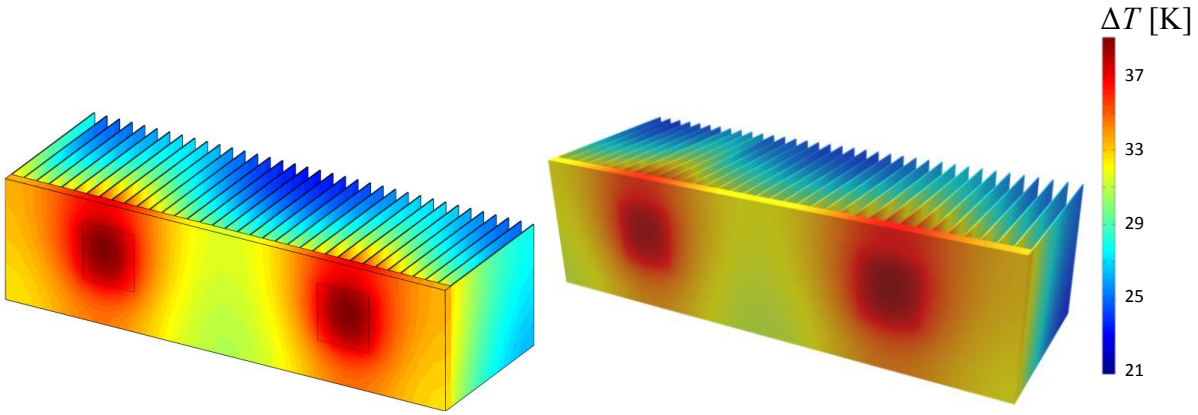

Figure 7. Temperature field with the new model (left) and CFD (right)

6. Optimization results

6.1. Minimizing outer volume and mass

Optimization results are shown in figures 5 and 6. The shape of the Pareto-optimal solutions set in figure 5 is not perfectly smooth, perhaps because the discrete design variable N, i.e., the number of fins, may have caused the steps. Another reason may be the MOPSO optimization algorithm, which is not gradient-based and thus does not always find exactly optimum solutions but solutions near the optimal set. Yet—for practical purposes—nearby optimal solutions are very useful.

The final chosen optimum geometry on the right in figure 6 was also analyzed with CFD. The temperature fields of our model and those of CFD are shown in figure 7, where the left heat sink is the same as in figure 6. The symmetrical component locations in final geometry are 53 mm from the heat sink side edge and 38 mm from the bottom edge. Other dimensions are shown in table 3. The maximum temperatures are almost the same, whereas the minimum temperatures vary, because the

flow may enter from the tips of the fins in the CFD solution, whereas in our model the flow in the channels is always one-dimensional.

Table 3. Dimensions of the optimized case (from figure 7)

L [mm]	W [mm]	l [mm]	t [mm]	N [-]	b [mm]
68	256	82	0.54	36	6

7. Conclusions

This paper introduces a new heat transfer model, which can be used in optimization of a fin array cooled by natural convection. The model was tested by comparing its results with those of an isothermal 2D channel in the literature and with our CFD results with the OpenFOAM. Furthermore, a 3D reference array with two heat generating components was calculated with new model and compared to numerically modelled CFD results. After these verification tests, the mass and size of the reference 3D array were simultaneously optimized using this proposed model when the component maximum temperatures were fixed.

The new model is many orders of magnitude faster than a CFD solution, which cannot be practically used for multi-objective optimization of applications. The test proved the usefulness of our model in multi-objective optimization process.

8. References

[1] Elenbaas W 1942 Heat Dissipation of Parallel Plates by Free Convection *Physica*, **9**(1) 665 – 671

[2] Bar-Cohen A and Rohsenow W 1984 Thermally Optimum Spacing of Vertical, Natural Convection Cooled, Parallel Plates *ASME J. Heat Transfer* **106** 116 – 122

[3] Aihara T 1991 Air Cooling Techniques by Natural Convection, Cooling Techniques for Computers, ed W Aung, (New York: Hemisphere) 1–45

[4] Raithby G D and Hollands K G T 1985 *Natural Convection, Handbook of Heat Transfer Fundamentals, 2nd ed.*, ed W M Rohsenow et. al, (New York: McGraw–Hill) chapter 6 pp 6-37

[5] Yovanovich M M, Teertstra P 2002 Natural convection Inside Vertical Isothermal Ducts of Constant Arbitrary Cross Section *Journal of Thermophysics and Heat Transfer* **16**(1)

[6] Lee S and Yovanovich M 1993 Linearization method for buoyancy induced flow over a nonisothermal vertical plate *J. Thermophys. Heat Transfer* **7** 158-164

[7] Karvinen R and Lampio K October 18-21 2013 Multi-objective optimization of electronics heat sink geometries (Invited paper) *Proc. of IWHT 2013 (Xi'an, China)*

[8] Lindstedt M, Lampio K, Karvinen R 2015 Optimal shapes of straight fins and finned heat sinks *ASME J. Heat Transfer* **137**(6) 061006-1-8

[9] Shah R K and London A L 1978 *Laminar flow Forced Convection in ducts*, (New York: Academic Press)

[10] Coello Coello C, Pulido G, Lechuga M 2004 Handling multiple objectives with particle swarm optimization *IEEE Transactions on evolutionary computation* **8**(3)